Journal of Bionic Engineering (2023) 20:1626–1634
https://doi.org/10.1007/s42235-023-00353-x

RESEARCH ARTICLE

Coiled Polymer Artificial Muscles Having Dual-Mode Actuation with Large Stress Generation

Xinghao Hu[1] · Runmin Liu[1] · Kai Zhao[1] · Yilun Wang[1] · Xianfu Bao[1] · Lin Xu[1] · Guanggui Cheng[1] · Jianning Ding[1,2]

Received: 5 November 2022 / Revised: 27 January 2023 / Accepted: 1 February 2023 / Published online: 15 February 2023

Abstract

Coiled polymer artificial muscles with both large tensile stroke and giant force generation are needed for practical applications in robotics, soft exosuits, and prosthesis. However, most polymer yarn artificial muscles cannot generate a large force or stress. Here, we report an inexpensive Twisted and Coiled Polymer artificial muscle (TCP) that performs both large isobaric and isometric contractions. This TCP can generate a tensile stroke of 20.1% and a specific work capacity of up to 1.3 kJ kg^{-1} during temperature changes from 20 to 180 °C. Moreover, the nylon yarn artificial muscle produced a reversible output stress of 28.4 MPa, which is 100 times larger than human skeletal muscle. A robot arm and a simple gripper were made to demonstrate the isobaric actuation and isometric actuation of our TCP muscle, repectivley. Thus, the polymer artificial muscles with dual-mode actuation show potential applications in the field of robotics, grippers, and exoskeletons and so on.

Keywords Coiled nylon muscles · Dual-mode actuation · Large stroke · Stress generation

1 Introduction

Artificial muscles, which can transfer other types of energies (such as thermal and electrothermal energy) to mechanical energy, have received extensive attention in multiple fields ranging from material science, mechanical and medical engineering as well as robotics [1]. Ideal artificial muscles should have a performance like high energy conversion efficiency, fast response, scalability, non-hysteretic, long-cycle life and low cost, and so on. Various types of artificial muscles such as pneumatic actuators [2], electroactive polymer (EAP) actuators, shape memory polymers (SMPs), and carbon nanotube (CNT)-based actuators have been developed [3–6]. However, most of the existing artificial muscles are suffering from some problems. For example, various pneumatic muscles provide fast actuation and large contraction strain, but they need extra pumps and valves, which make the system bulky [7–9]. The dielectric elastomers can actuate rapidly (over 100 Hz), but they should be stimulated at a high voltage of 2–20 kV [10–13]. While thermally driven SMAs have fast actuation rate and generate large force, the high cost and large hysteresis of SMA also hamper their extensive applications [14].

Recently, a twisted and coiled soft actuator using inexpensive polymer fibers (such as nylon, Kevlar, polyethylene, etc.) was developed [15, 16], which can provide high power density, large stroke, low hysteresis, and considerable repeatability. The twisted nylon fiber artificial muscle will untwist when driven thermally due to its anisotropic thermal expansion coefficient [17]. This allows for both torsional and tensile actuation due to its coiled-structure frame [18]. For more practical applications, the nonconductive nylon muscle could be electrothermally driven by different approaches, for instance, wrapping nylon fiber with flexible carbon nanotube sheets [19], coating nylon fiber with conductive silver paint [20], and by twisting metal wire and fishing line simultaneously [21, 22]. From the viewpoint of muscle physiology, contraction is not only limited to the shortening of muscle length, i.e. isobaric contraction, but also means that a force can be produced in isometric conditions without length change. However, traditional nylon artificial muscles normally

✉ Xinghao Hu
huxh@ujs.edu.cn

✉ Jianning Ding
dingjn@ujs.edu.cn

[1] Institute of Intelligent Flexible Mechatronics, School of Mechanical Engineering, Jiangsu University, Zhenjiang 212013, China

[2] School of Mechanical Engineering, Yangzhou University, Yangzhou 225009, China

deal with isobaric movement only, other functions are simply neglected in various types of materials.

In the present work, we report a twisted and coiled nylon artificial muscle that performs both isobaric and isometric contractions (means dual-mode actuation). This muscle contracts in response to the temperature change of the muscle. As a result, a tensile stroke of higher than 20.1% and a specific work capacity of up to 1.3 kJ kg^{-1} were obtained during temperature changes from 20 to 180 °C, respectively. By wrapping a conductive copper wire, this muscle can operate at relatively low voltages (≤ 1 V), and the stroke is proved to reversibly and linearly respond to the applied voltages. In addition, the nylon yarn artificial muscle can produce reversible output stress of 28.4 MPa, which is 100 times higher than human skeletal muscle. Thus, the polymer artificial muscles with dual-mode actuation show potential applications in the field of robotics, grippers and exoskeletons and so on.

2 Experimental Sections

2.1 Fabrication of Self-Coiled Nylon Muscles and Copper Wire-Wrapped Coiled Nylon Muscles

The monofilament nylon fiber was purchased from Statex Productions & Vertriebs GmbH (Shieldex PN# 260151011717 and 260151023534). Self-coiled nylon muscles were made by inserting twist into a nylon fiber. As shown in Fig. S1a, a nylon fiber was hung on a stepper motor, and a constant load was applied to the nylon fiber during the twisting process. To prevent the untwist of nylon yarn during actuation, it was torsionally tethered via a wood stick. By over-twisting, a fully coiled nylon muscle was made. A copper wire-wrapped coiled nylon fiber was made by wrapping a 50-μm-diameter copper wire with the coiled nylon fiber. To avoid the stroke restriction by copper wire, the wrapping direction was opposite to the coil direction (Fig. 2a). This thin copper wire has a negligible mechanical effect on the actuation.

Unless otherwise indicated, the tensile stroke is defined as the length change during actuation divided by the length of the loaded muscle. The applied tensile stress is the constant force normalized to the yarn diameter of the fully twisted yarn. The generated stress was calculated using the generated force divided by the cross-sectional area of the coiled muscle. Spring index C is defined in spring mechanics as $C = D/d$, where d is the fiber diameter and D is the nominal coil diameter as measured by the fiber centerline.

2.2 Characterizations

The morphology and structure of the coiled nylon yarn and the copper-wire-wrapped nylon yarn were obtained by scanning electron microscopy (SEM, model JSM-7800F, JEOL, Japan). The change in modulus and generated stress for the coiled nylon muscle with temperature was measured by thermomechanical analysis (TMA, TMA 7100, Hitachi, Japan). The change in the pitch of coiled nylon was observed by optical microscopy (DMi8, Leica, Germany). The temperature change of the coiled nylon muscle was recorded using a thermographic high-resolution system (T540, FLIR, United States). The mechanical properties of the nylon fiber were tested by a universal mechanical testing machine (5944, Instron, America).

3 Results and Discussion

3.1 Thermally Powered Self-Coiled Nylon Muscles

For thermally powered Twisted and Coiled Polymer (TCP) artificial muscles, the actuation mechanism is depicted in Fig. 1a. It illustrates that thermal expansion causes the yarn to untwist, which leads to yarn length contraction. Isobaric tensile actuation for thermally powered nylon 6,6 muscle was measured by thermal dynamic analysis (TMA). To achieve reversible actuation, the coiled nylon muscle has been thermally annealed at 150 °C for 0.5 h before actuation, and the working temperature was set from 20 to 180 °C at a rate of 10 °C min^{-1}. As a result, the tensile stroke as a function of temperature for the coiled nylon muscle was obtained (Fig. 1b). Yarn muscle monotonically contracts with increasing temperature for most applied mechanical loads. Notably, if the applied load is smaller than the load used for coiling, adjacent coils are in contact, limiting contraction during actuation. Thus, for the applied load of 5.4 MPa, yarn muscle first contracts with increasing temperature until a peak value of 14.5% was achieved, and keeps no change when continue increasing temperature. Increasing load can separate adjacent coils and achieve larger actuation. Figure 1c shows the load dependence of tensile stroke for the coiled nylon muscles. The tensile stroke increases with increasing applied tensile stress until a maximum value of 20.1% was achieved under an optimal load of 10.7 MPa. With increasing applied load, the muscle's initial length was stretched, leading to a decreased tensile stroke. The work capacity that nylon muscle generated during contraction monotonically increases with increasing applied tensile stress and reaches 1.3 J g^{-1} when the applied load was 31 MPa, which is 32 times that of mammal muscle [23].

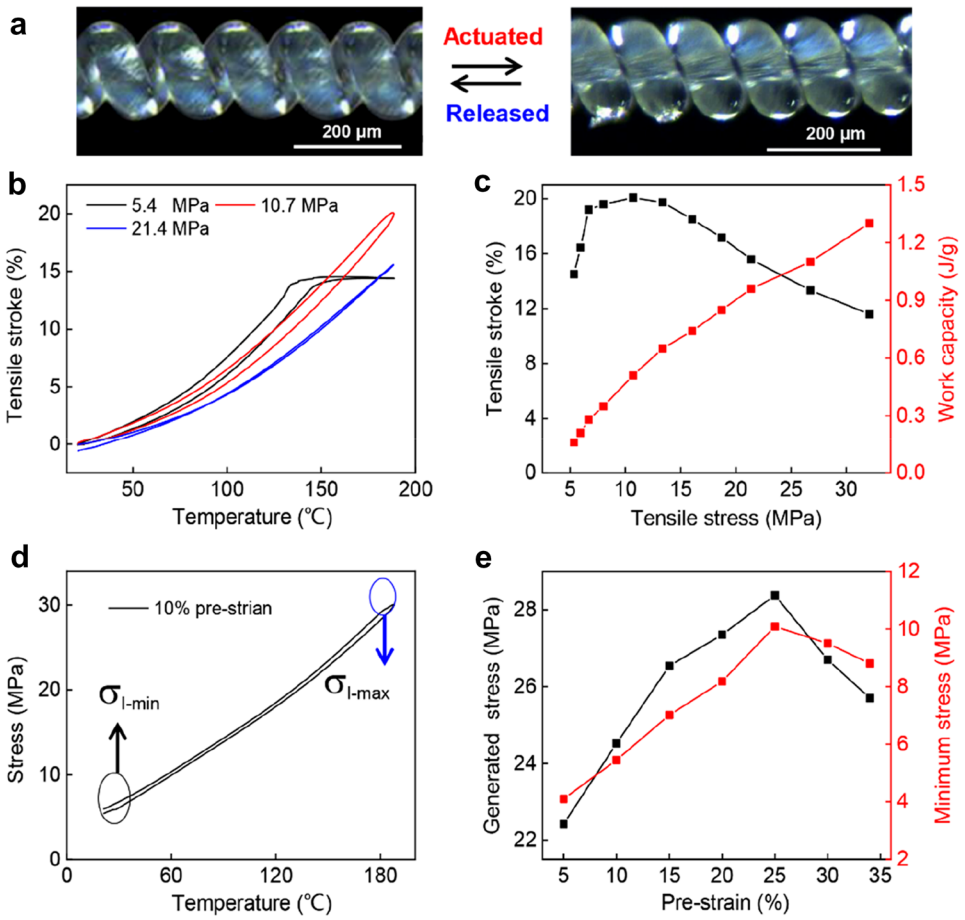

Fig. 1 Dual-mode actuation performance for a self-coiled nylon muscle. **a** Optical images of a coiled nylon muscle at un-actuated and actuated states. **b** The temperature dependence of tensile stroke for a coiled, 69-μm-diameter nylon muscle under different applied mechanical loads. The spring index, twist density, and twisting load are 1.3, 37 turns cm^{-1}, and 26.7 MPa, respectively. **c** Tensile stroke and work capacity as a function of applied tensile stress for the muscle used in (**b**). **d** The generated stress as a function of temperature under a pre-strain of 10% for the muscle used in (**b**). **e** The generated stress and initial stress ($\sigma_{I\text{-}min}$) as a function of applied pre-strain for the muscle used in (**d**)

From the aspect of natural muscle, the output performance is not only limited to the muscle length contraction, but also means that a force can be generated in isometric conditions without muscle length change [24]. When a nylon artificial muscle was thermally heated, the yarn muscle first absorbs thermal energy and then transmits the energy to the coiled structure. Consequently, an isometric force was generated. Isometric contraction is also an important parameter of a high-performance artificial muscle.

To mimic the isometric contraction, a similar setup was employed (as illustrated in fig. S1c) where the sample length is fixed, and stress evolution could be recorded by the load cell when external stimulation was applied. In each experiment, the specimen was subjected to at least three consecutive thermal cycles where stress can be significantly produced in heating and elapse in cooling. By applying a pre-strain of 10%, nylon muscle produced initial stress ($\sigma_{I\text{-}min}$), and the stress increases with increasing temperature until a maximum value ($\sigma_{I\text{-}max}$) was achieved (Fig. 1d). With an increase in pre-strains, both the maximum and minimum isometric stress increase accordingly (fig. S2), from 4.1 to 10.1 MPa of $\sigma_{I\text{-}min}$. The generated stress was calculated by the difference between $\sigma_{I\text{-}max}$ and $\sigma_{I\text{-}min}$. For each pre-strain, $\sigma_{I\text{-}min}$ and $\sigma_{I\text{-}max}$ stay at the same level despite the number of cycles. With an increase in strains, the value and variation mode of stress is observed to strongly depend on the pre-strains, reflecting the effect of crystallization behavior and thermodynamic properties on contraction performance [25]. The stress generation as a function of the applied pre-strain was shown in Fig. 1e. It is worth noting that nylon muscle can produce more than 28 MPa stress under 25% pre-strain, which is more than 3.5 times than for CNT-NCY hybrid muscle [26] and 100 times than for human muscle [23] (~0.3 MPa).

3.2 Electrothermally Powered Copper Wire-Wrapped Coiled Nylon Muscles

3.2.1 Isobaric Actuation

Although self-coiled nylon muscles can achieve excellent actuation performance, they cannot be powered by electricity due to their non-conductivity. By wrapping coiled nylon fiber with a copper wire, we made an electrothermally powered nylon muscle. To avoid the stroke restriction by copper wire, the wrapping direction was opposite to the coil

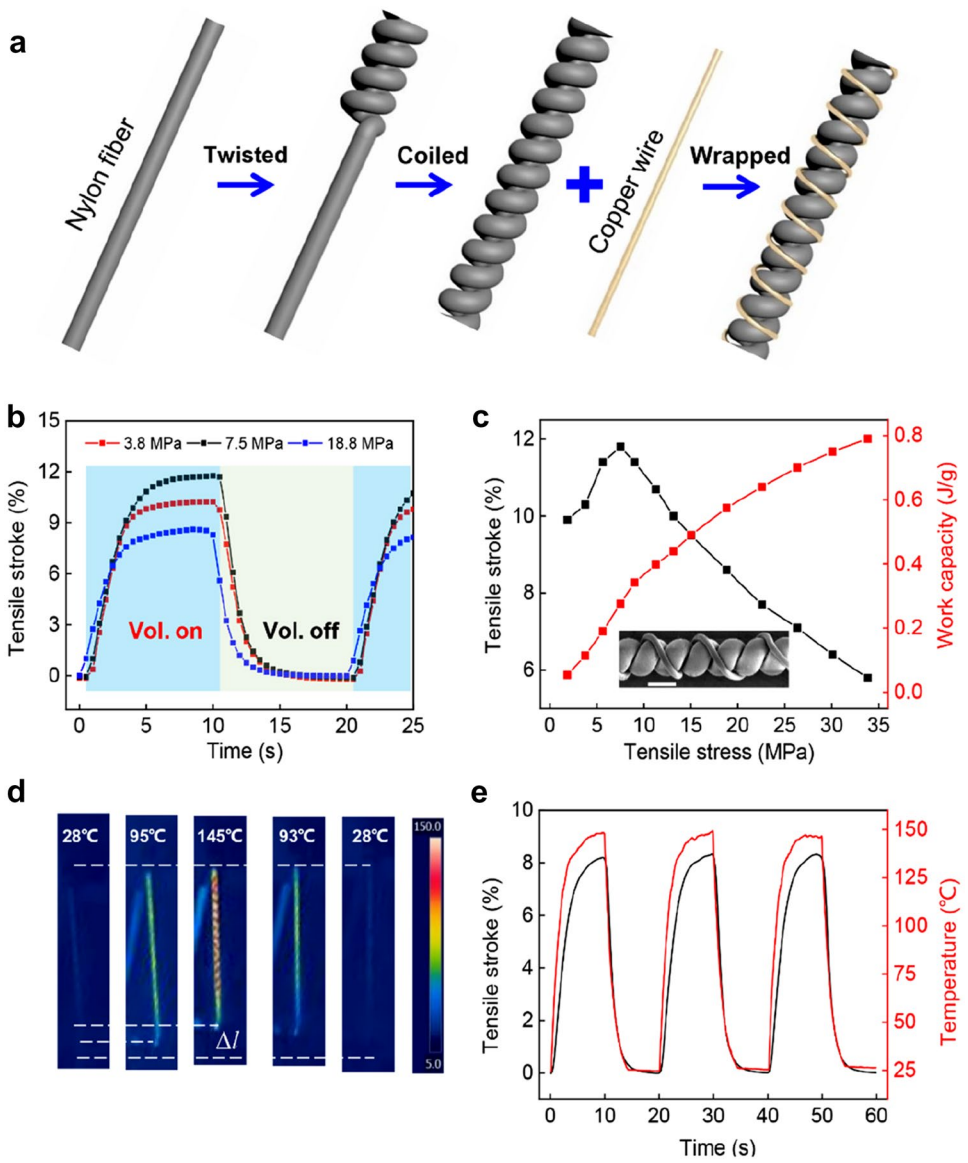

Fig. 2 Isobaric actuation for an electrothermally powered nylon muscle. **a** Schematic illustration of the fabrication method for a coiled, copper-wire-wrapped nylon muscle. **b** Tensile stroke as a function of time for a coiled, copper wire-wrapped, 130-μm-diameter nylon muscle under different applied tensile stresses. **c** Tensile stroke and work capacity as a function of applied tensile stress for the muscle used in (**b**). Inset shows the SEM image for the copper wire-wrapped nylon muscle. The scale bar is 200 μm. **d** Thermal camera images show the temperature change for the coiled nylon muscle when driven by a 0.05 Hz, 0.23 W cm^{-1} square-ware voltage with a 50% duty cycle. **e** The time dependence of isobaric tensile stroke (left *y*-axis) at applied tensile stress of 10.5 MPa and the real-time temperature (right y-axis) for the electrothermally driven nylon muscle used in (**d**)

direction (Fig. 2a). Also, the winding density (the number of winding turns divided by the total muscle length) of copper wire would affect the uniformity of thermal energy on the yarn muscle that delivered by electrical power. Figure 2b shows the tensile stroke as a function of time under different applied loads. During a heating–cooling cycle, muscle contracts to a maximum value within 4.5 s, and provide a large stroke rate of 2.2% s^{-1}. The load dependence of the tensile stroke and work capacity for electrothermally powered nylon muscle has also been obtained (Fig. 2c). By applying a 0.28 W cm^{-1} square-wave voltage, nylon muscle can generate a maximum tensile stroke of 12.1% and a work capacity of 0.8 J g^{-1}, respectively. After the wrapping process, we measured the real-time temperature using a thermal camera during the nylon muscle contraction, which is shown in Fig. 2d. It depicts that the nylon yarn muscle was uniformly heated by electrical power. In addition, the real-time temperature of yarn muscle exhibits the same trend with tensile stroke (Fig. 2e).

The actuation performance for electrothermally powered nylon muscle can be improved by varying actuation frequency, duty cycle, and input power. Figure 3a demonstrates the tensile stroke changes with time under different applied frequencies. The applied tensile stress and power were 8.6 MPa and 0.27 W cm^{-1} square wave, respectively. At a low frequency of 0.02 Hz, nylon muscle generates a maximum tensile stroke of 11.6%. While at a high frequency of 0.5 Hz, nylon muscle contracts insufficiently in the first cycle and quickly increased to the stabilized stroke after a few cycles. Due to the limited time to cool at high frequencies, nylon muscle cannot release back to its original length and only actuated at high-temperature regions.

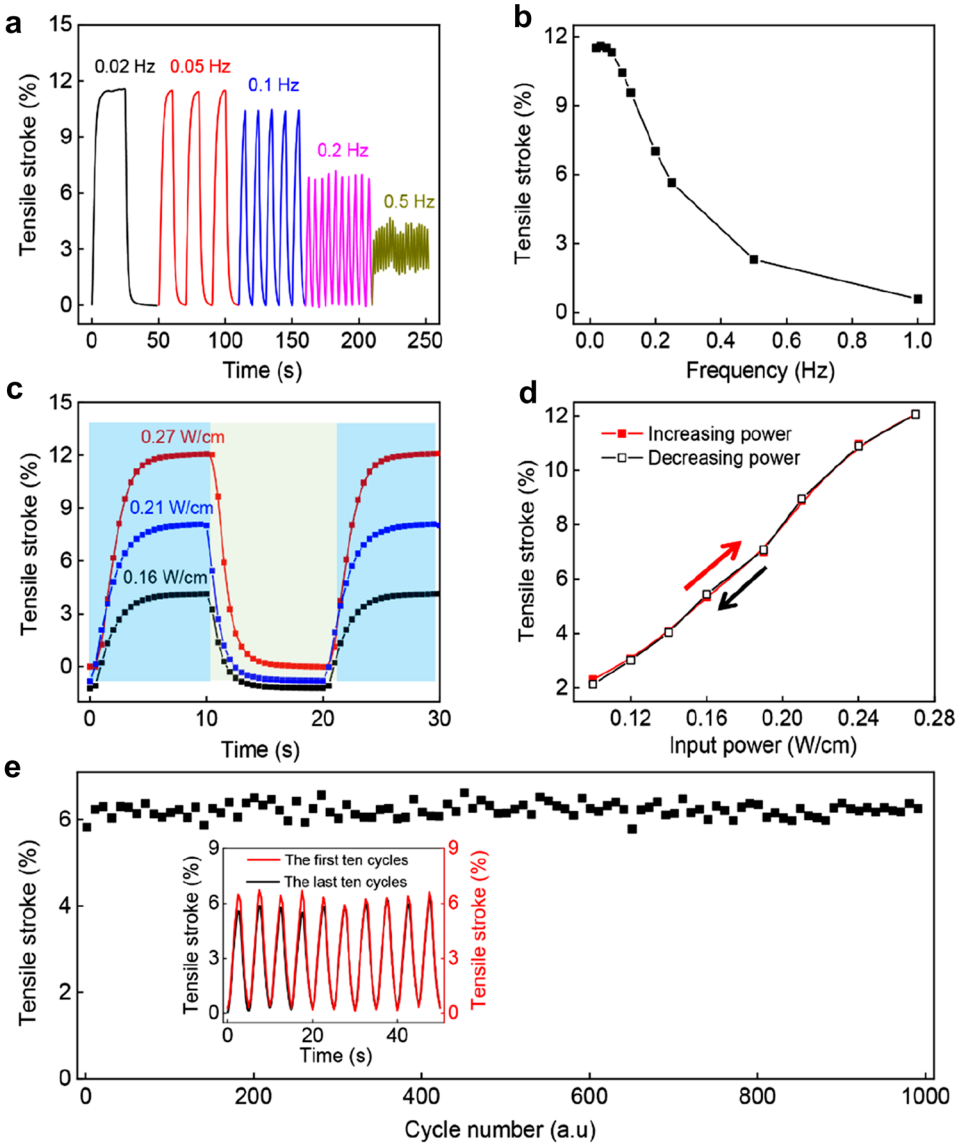

Fig. 3 Impact factors of isobaric actuation for an electrothermally powered nylon muscle. **a** Time dependence of tensile stroke for a coiled, copper-wrapped, 130-μm-diameter nylon muscle under different applied frequencies. The applied voltage and isobaric tensile stress were 0.27 W cm^{-1}, 8.6 MPa respectively. **b** Tensile stroke as a function of applied square wave frequency for the muscle used in (**a**). **c** Tensile stroke versus time under different input power densities with the same frequency of 0.05 Hz for the muscle used in (**a**). The applied tensile stress was 8.6 MPa. **d** Tensile stroke as a function of input power at 0.05 Hz, 50% duty cycle square wave voltage. **e** Tensile stroke versus cycle for the muscle in (**a**) when driven electrothermally at 0.2 Hz, 50% duty cycle, 0.21 W cm^{-1} square wave voltage under a 7.5-MPa load. Inset shows the stroke change of the first 10 cycles and the last 10 cycles for the coiled nylon muscle

Consequently, muscle stroke decreased with the increase in frequency (Fig. 3b). Besides, the yarn's diameter also affects the actuation for different frequencies, especially for high frequencies. As shown in Fig. S6b, the cooling time (defined as the time needed to reduce the tensile stroke by 90%. [3]) for an 80-μm-diameter nylon muscle (1.9 s) is much shorter than for a 200-μm-diameter nylon muscle (7.2 s), indicating that muscles with a small diameter can be cycled at a higher frequency than for a larger one (Fig. S6b).

Note that the contractile rate (tensile stroke divided by the contractile time) and release rate (tensile stroke divided by the release time) are not always matched. Thus, the duty cycle would also affect the actuation performance. Fig. S3a shows the duty cycle dependence of the tensile stroke for a coiled nylon muscle measured at a 0.05 Hz, 0.28 W cm^{-1} square-wave power. At a low duty cycle of 10%, the heating time is too short, which limited the input electrothermal energy, leading to a small contractile stroke. At a high duty cycle of 90%, the cooling time is too short, which made yarn muscle fail to return to its original state, causing the decrease of absolute tensile stroke. Consequently, an appropriate duty cycle is necessary to achieve the largest tensile actuation. After varying different duty cycles, we found that the maximum tensile stroke is 12% at the optimal duty cycle of 50%. Thus, the tensile stroke increased first with the increment of the duty cycle and then decreased after it reached the maximum value, as shown in Fig. S3b.

More importantly, the input power and cycle stability of muscle are significant for practice use [27]. We have measured the dependence of tensile stroke on the input power density, which is illustrated in Fig. 3c, d. The tensile stroke increases almost linearly and reversibly with the input power

density. Typically, the tensile stroke increases from 4.1% at an input power of 0.16 W cm^{-1} to 12.1% at an input power of 0.27 W cm^{-1}. The cycle stability of electrothermally powered copper wire-wrapped nylon muscle has also been measured. As shown in Fig. 3e, the nylon muscle provides a very stable contraction stroke for at least 1000 cycles when a 0.2 Hz, 50% duty cycle, 0.25 W cm^{-1} square-wave power was applied. Thus, the electrothermally powered nylon muscle are feasible material for the applications of soft robotics and exosuits. In addition, we have demonstrated the potential application of a copper-wire wrapped nylon artificial muscle lifting heavy weight when electrothermally driven at a 0.05 Hz, 50% duty cycle, and 6.5 V square-wave voltage (shown in Movie S1).

3.2.2 Isometric Actuation

Similar to the self-coiled nylon muscle, the generated isometric stress of a coiled, copper wire-wrapped nylon muscle has been investigated. The muscle was fixed in a tensile dynamometer with two ends clamped and connected by an electrical wire to a power supply (Fig. S1b). Fig. S4a shows the time dependence of the generated stress of the coiled, copper wire-wrapped nylon muscle under different applied preload strains. The input electrical power was 0.05 Hz, 0.27 W cm^{-1} square-wave with 50% duty cycle. When the voltage was applied to the nylon muscle, the generated isometric stress increased rapidly and then sluggishly increase to the maximum value. When the applied voltage was switched to 0 V, the generated stress gradually decreased to the initial stress. Figure 4a shows that the generated isometric stress first increased with the increase in the pre-strain and then reached a maximum value of 28.4 MPa at the pre-strain of 25%.

The frequency, input power, and duty cycle dependence of generated isometric stress for the electrothermally powered nylon muscle were also measured. Figure 4b shows the dependence of the isometric stress of the electrothermally powered nylon muscle under different frequencies driven by an input power of 0.19 W cm^{-1} at 10% pre-strain. With the increase in applied frequency, the generated stress decreases because of insufficient heating time. Typically, the generated stress of 15 MPa at a frequency of 0.05 Hz decreased to 1 MPa at a frequency of 1 Hz. Notably, even if the applied frequency is as high as 1 Hz, the nylon muscle can still generate an isometric stress of 1 MPa, which is higher than some of the electrochemical-powered artificial muscles [such as Bucky gel (=0.1 MPa)] [28]. Moreover, the generated isometric stress can be improved by increasing input power. We have measured the generated stress under different input powers when driven at 0.05 Hz square wave voltage for the applied pre-strain of 10% (Fig. S4b). The generated stress increases approximately linearly with input power (Fig. 4c). Typically, yarn muscle can generate isometric stress of 23.6 MPa when an input power of 0.3 W cm^{-1} was applied. In addition, the optimal duty cycle is also needed to achieve large stress. At a small duty cycle, laking of heating time, the muscle cannot reach the maximum final generated stress; while at a higher duty cycle, lacking of cooling time, the minimum initial generated stress cannot be reached. Therefore, when the 50% duty cycle was applied, the maximum stress peak intensity reached 23.8 MPa (fig. S3c–3d).

The generated isometric stress of coiled nylon muscles can be changed by adjusting the spring index of the coiled structure. The spring index C is defined as the yarn diameter divided by the fiber diameter, and it can significantly affect the actuation performance [18]. Figure 4d shows the pre-strain dependence of generated stress for coils with spring index of 1.35, 1.23, and 1.12, fabricated by coiling under the stress of 16.9, 28.2, and 39.5 MPa, respectively. It shows that the generated stress decreases with increasing spring index. It is reasonable because a muscle with a large spring index has a small modulus [14]. For the minimum spring index ($C=1.12$), the maximum generated isometric stress reached 23 MPa when the 20% tensile pre-strain was applied.

The output stress stability of the coiled nylon muscle was also tested. The nylon muscle was stimulated by a 0.3 W cm^{-1}, 0.1 Hz square wave voltage under a preload strain of 10%. Figure 4e shows that yarn muscle produces a stable output stress at least for 1000 cycles, the generated stress decreased by 26% after 1000 cycles. Figure 4f compares the tensile stroke and generated isometric stresses by our nylon yarn muscles with mammalian skeletal muscles and previously reported fiber-based artificial muscles. Some muscles can generate a large tensile stroke, but they can only provide a small generated stress. For example, natural muscles like wool yarn, flax yarn, and cotton yarn generate a maximum tensile stroke and stress of 39%, 17%, 18% and 2.6, 8.5, 9 MPa, respectively [31]. Most polymer-based fiber muscles like poly(ε-caprolactone)-based polyurethane (PCL) muscle can generate a large stroke but small stress [24]. Our nylon yarn muscle can generate an isometric stress of 28.4 MPa, which is more than 100 times that of mammalian skeletal muscles (≈0.35 MPa) [29], and provide a large tensile stroke of 20.1% with a work capacity of 1.3 kJ kg^{-1}.

When a nylon muscle generates stress at a fixed length, the stiffness of the muscle is also changed (Fig. S5a). Thus, the isometric contraction is related to the muscle's stiffness variation. Based on this concept, a gripper made of four copper wire-wrapped nylon muscles was designed to demonstrate the applications of isometric contraction. As shown in Movie S2, firstly the gripper cannot lift a 30 g bottle when the muscle was close contact with the bottle (shown in Fig S7). Once a 19 V voltage was applied, nylon muscles generate a large force (F_1, F_2), inducing an extra pressure force

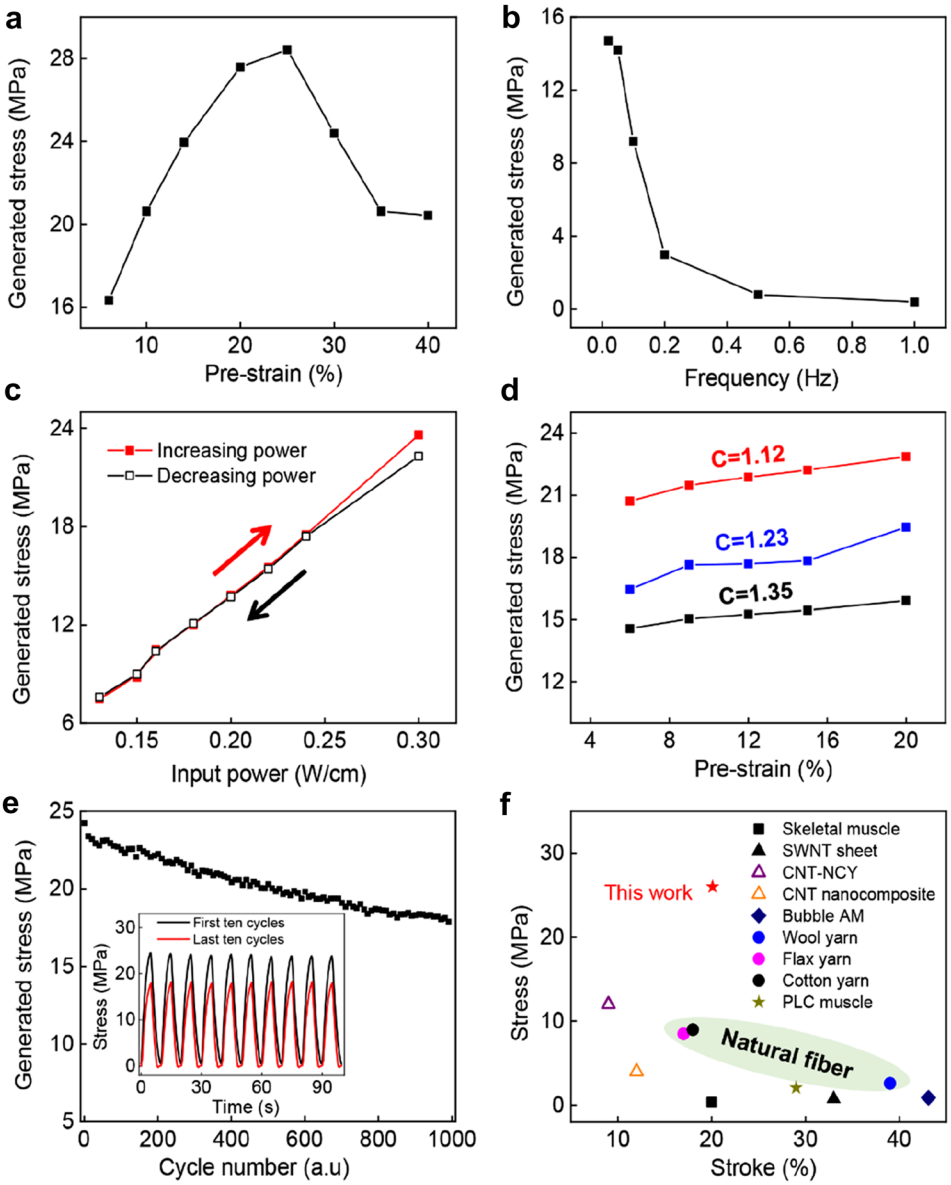

Fig. 4 Impact factors of isometric actuation for an electrothermally powered nylon muscle. **a** Stress generation versus applied pre-strains for a coiled, copper wire-wrapped, 130-μm-diameter nylon muscle. **b** The generated stress as a function of applied frequency for the muscle used in (**a**). **c** Stress as a function of input power at 0.05 Hz, 50% duty cycle square-wave voltage. **d** The generated stress as a function of pre-strain for the muscles with different spring indexes of 1.12, 1.23, and 1.35. **e** The cycle stability of generated stress for the muscle used in (**a**) under 10% pre-strain when driven by a 0.1 Hz, 0.3 W cm^{-1} square wave voltage. **f** Comparison of tensile stroke and the generated isometric stress with mammalian skeletal muscles (20%, 0.75 MPa) [29], SWNT sheet (33%, ~ 0.75 MPa) [30], CNT-NCY yarn muscle (9%, 12 MPa) [26], CNT composite yarn muscle (12%, 4 MPa) [27], Wool yarn (39%, ~ 2.6 MPa) [31], Flax yarn (17%, ~ 8.5 MPa) [31], Catton yarn (18%, ~ 9 MPa) [31] and poly(ε-caprolactone)-based polyurethane (PCL) muscle (29%, 2.08 MPa) [32]

($F_{1y}+F_{2y}$) and a friction force of μ($F_{1y}+F_{2y}$) (where μ is friction coefficient) on the bottle. As a result, the gripper can easily pick up the bottle when applied external voltage. During the whole process, the length of the muscle was fixed. Thus, isometric contraction plays an important role in robotic application that needs to vary their stiffness, such as grippers and variable wings.

4 Conclusion

Many types of artificial muscle can provide large stroke and work capacity, but generate small stress for isometric conditions. In this work, we developed an inexpensive twisted and coiled nylon artificial muscle that performs large dual-mode actuation of isobaric and isometric contractions. This TCP contracts responsive to temperature change with a tensile stroke higher than 20.1%, and a specific work up to 1.3 kJ kg^{-1}, respectively. By wrapping a conductive wire, this TCP can work at low voltages (≤ 1 V), and the stroke is proved to reversibly and linearly respond to the applied voltages. Moreover, the coiled nylon yarn artificial muscle can produce a reversible output stress of 26 MPa, which is more than 100 times higher than human skeletal muscle. Thus, this soft nylon muscle realizes the significant multifunction of an artificial muscle.

Supplementary Information The online version contains supplementary material available at https://doi.org/10.1007/s42235-023-00353-x.

Acknowledgements Financial support from the program of the National Natural Science Foundation of China (Grant no. 52105057, 51905222), Natural Science Foundation of Jiangsu Province (Grant no. BK20200916), China Postdoctoral Science Foundation (no. 2021M691307, no. 2022T150274), Jiangsu Postdoctoral Research Foundation (no. 2021K543C), Key Research Project of Zhejiang Lab, and Senior Talent Foundation of Jiangsu University (Grant no. 5501110013) are acknowledged.

Data Availability The data used to support the results of this study are available from the corresponding author upon reasonable request.

Declarations

Conflict of Interest The authors declare no conflict of interest.

References

1. Mirvakili, S. M., & Hunter, I. W. (2018). Artificial muscles: Mechanisms, applications, and challenges. *Advanced Materials, 30*, 1704407.
2. Xiao, W., Hu, D., Chen, W. X., Yang, G., & Han, X. (2021). Design, characterization, and optimization of multi-directional bending pneumatic artificial muscles. *Journal of Bionic Engineering, 18*, 1358–1368.
3. Hu, X. H., Jia, J. J., Wang, Y. M., Tang, X. T., Fang, S. L., Wang, Y. L., Baughman, R. H., & Ding, J. N. (2022). Fast large-stroke sheath-driven electrothermal artificial muscles with high power densities. *Advanced Functional Materials, 32*, 2200591.
4. Dai, S. P., Zhou, X. S., Hu, X. H., Dong, X., Jiang, Y. Y., Cheng, G. G., Yuan, N. Y., & Ding, J. N. (2021). Carbon nanotube hybrid yarn with mechanically strong healable silicone elastomers for artificial muscle. *ACS Applied Nano Materials, 4*, 5123–5130.
5. Chu, H. T., Hu, X. H., Wang, Z., Mu, J. K., Li, N., Zhou, X. S., Fang, S. L., Haines, C. S., Park, J. W., Qin, S., Yuan, N. Y., Xu, J., Tawfick, S., Kim, H. J., Conlin, P., Cho, M., Cho, K., Oh, J. Y., Nielsen, S., … Baughman, R. H. (2021). Unipolar stroke, electroosmotic pump carbon nanotube yarn muscles. *Science, 371*, 494–498.
6. Ren, M., Qiao, J., Wang, Y. L., Wu, K. J., Dong, L. Z., Shen, X. F., Zhang, H. C., Yang, W., Wu, Y. L., Yong, Z. Z., Chen, W., Zhang, Y. Y., Di, J. T., & Li, Q. W. (2021). Strong and robust electrochemical artificial muscles by ionic-liquid-in-nanofiber-sheathed carbon nanotube yarns. *Small (Weinheim an der Bergstrasse, Germany), 17*, 2006181.
7. Li, S. G., Vogt, D. M., Rus, D., & Wood, R. J. (2017). Fluid-driven origami-inspired artificial muscles. *Proceedings of the National Academy of Sciences, 114*, 13132–13137.
8. Guan, Q. H., Sun, J., Liu, Y. J., Wereley, N. M., & Leng, J. S. (2020). Novel bending and helical extensile/contractile pneumatic artificial muscles inspired by elephant trunk. *Soft Robotics, 7*, 597–614.
9. Mirvakili, S. M., Sim, D., Hunter, I. W., & Langer, R. (2020). Actuation of untethered pneumatic artificial muscles and soft robots using magnetically induced liquid-to-gas phase transitions. *Science Robotics, 5*, eaaz4239.
10. Li, T. F., Li, G. R., Liang, Y. M., Cheng, T. Y., Dai, J., Yang, X. X., Liu, B. Y., Zeng, Z. D., Huang, Z. L., & Luo, Y. W. (2017). Fast-moving soft electronic fish. *Science Advances, 3*, e1602045.
11. Kellaris, N., Gopaluni, V. V., Smith, G. M., Mitchell, S. K., & Keplinger, C. (2018). Peano-HASEL actuators: Muscle-mimetic, electrohydraulic transducers that linearly contract on activation. *Science Robotics, 3*, eaar3276.
12. Duduta, M., Hajiesmaili, E., Zhao, H. C., Wood, R. J., & Clarke, D. R. (2019). Realizing the potential of dielectric elastomer artificial muscles. *Proceedings of the National Academy of Sciences, 116*, 2476–2481.
13. Zhang, Y., Ellingford, C., Zhang, R. N., Roscow, J., Hopkins, M., Keogh, P., McNally, T., Bowen, C., & Wan, C. Y. (2019). Electrical and mechanical self-healing in high-performance dielectric elastomer actuator materials. *Advanced Functional Materials, 29*, 1808431.
14. Thomas, S., Germano, P., Martinez, T., & Perriard, Y. (2021). An untethered mechanically-intelligent inchworm robot powered by a shape memory alloy oscillator. *Sensors and Actuators A, 332*, 113115.
15. Haines, C. S., Lima, M. D., Li, N., Spinks, G. M., Foroughi, J., Madden, J. D., Kim, S. H., Fang, S. L., Jung de Andrade, M., Göktepe, F., Göktepe, Ö., Mirvakili, S. M., Naficy, S., Lepró, X., Oh, J. Y., Kozlov, M. E., Kim, S. J., Xu, X. R., Swedlove, B. J., … Baughman, R. H. (2014). Artificial muscles from fishing line and sewing thread. *Science, 343*, 868–872.
16. Park, J., Yoo, J. W., Seo, H. W., Lee, Y., Suhr, J., Moon, H., Koo, J. C., Choi, H. R., Hunt, R., Kim, K. J., Kim, S. H., & Nam, J. D. (2017). Electrically controllable twisted-coiled artificial muscle actuators using surface-modified polyester fibers. *Smart Materials and Structures, 26*, 035048.
17. Tang, X. T., Li, K., Liu, Y. X., Zhou, D., & Zhao, J. G. (2019). A general soft robot module driven by twisted and coiled actuators. *Smart Materials and Structures, 28*, 035019.
18. Aziz, S., Naficy, S., Foroughi, J., Brown, H. R., & Spinks, G. M. (2017). Thermomechanical effects in the torsional actuation of twisted nylon 6 fiber. *Journal of Applied Polymer Science, 134*, 45529.
19. Liu, Z. F., Fang, S. L., Moura, F., Ding, J. N., Jiang, N., Di, J., Zhang, M., Lepró, X., Galvao, D., Haines, C. S., Yuan, N. Y., Yin, S. G., Lee, D. W., Wang, R., Wang, H. Y., Lv, W., Dong, C., Zhang, R. C., Chen, M. J., … Baughman, R. H. (2015). Hierarchically buckled sheath-core fibers for superelastic electronics, sensors, and muscles. *Science, 349*, 400–404.
20. Wu, L. J., Chauhan, I., & Tadesse, Y. (2018). A novel soft actuator for the musculoskeletal system. *Advanced Materials Technologies, 3*, 1700359.
21. Xiang, C. Q., Yang, H., Sun, Z. Y., Xue, B. C., Hao, L. N., Rahoman, M. A., & Davis, S. (2017). The design, hysteresis modeling and control of a novel SMA-fishing-line actuator. *Smart Materials and Structures, 26*, 037004.
22. Helps, T., Taghavi, M., Wang, S. H., & Rossiter, J. (2020). Twisted rubber variable-stiffness artificial muscles. *Soft Robotics, 7*, 386–395.
23. Oguntosin, V., & Akindele, A. (2019). Design and characterization of artificial muscles from wedge-like pneumatic soft modules. *Sensors and Actuators A: Physical, 297*, 111523.

24. Zhu, S. S., Hu, J. L., & Zhang, Y. C. (2019). A single polymer artificial muscle having dual-mode contractibility, temperature sensibility, and trainability through enthalpy change. *Advanced Materials Technologies, 4*, 1900017.
25. Bhatti, M. R. A., Bilotti, E., Zhang, H., Varghese, S., Verpaalen, R. C., Schenning, A. P., Bastiaansen, C. W., & Peijs, T. (2020). Ultra-high actuation stress polymer actuators as light-driven artificial muscles. *ACS Applied Materials & Interfaces, 12*, 33210–33218.
26. Xu, L. L., Peng, Q. Y., Zhao, X., Li, P. Y., Xu, J. H., & He, X. D. (2020). A photoactuator based on stiffness-variable carbon nanotube nanocomposite yarn. *ACS Applied Materials & Interfaces, 12*, 40711–40718.
27. Xu, L. L., Peng, Q. Y., Zhu, Y., Zhao, X., Yang, M. L., Wang, S. S., Xue, F. H., Yuan, Y., Lin, Z. S., Xu, F., Sun, X. X., Li, J. J., Yin, W. L., Li, Y. B., & He, X. D. (2019). Artificial muscle with reversible and controllable deformation based on stiffness-variable carbon nanotube spring-like nanocomposite yarn. *Nanoscale, 11*, 8124–8132.
28. Fukushima, T., Asaka, K., Kosaka, A., & Aida, T. (2005). Fully plastic actuator through layer-by-layer casting with ionic-liquid-based bucky gel. *Angewandte Chemie International Edition, 44*, 2410–2413.
29. Baughman, R. H. (2005). Playing nature's game with artificial muscles. *Science, 308*, 63–65.
30. Baughman, R. H., Cui, C., Zakhidov, A. A., Iqbal, Z., Barisci, J. N., Spinks, G. M., Wallace, G. G., Mazzoldi, A., De Rossi, D., Rinzler, A. G., Jaschinski, O., Roth, S., & Kertesz, M. (1999). Carbon nanotube actuators. *Science, 284*, 1340–1344.
31. Yang, X. H., Wang, W. H., & Miao, M. H. (2018). Moisture-responsive natural fiber coil-structured artificial muscles. *ACS Applied Materials & Interfaces, 10*, 32256–32264.
32. Huang, L. B., Xie, X. X., Huang, H., Zhu, J., Yu, J. R., Wang, Y., & Hu, Z. M. (2020). Electrospun polyamide-6 nanofiber for hierarchically structured and multi-responsive actuator. *Senors and Actuators A*, *302*, 111793.